CO (J = 3 – 2) Emission in the Radio Galaxy 53W002 at z=2.394

N. Z. Scoville

California Institute of Technology, Pasadena, CA 91125

M. S. Yun

National Radio Astronomy Observatory, P.O. Box 0, Socorro, NM 87801

R. A. Windhorst

Department of Physics and Astronomy, Arizona State University, Box 871504, Tempe, AZ 85287-1504

W. C. Keel

Department of Physics and Astronomy, University of Alabama, Box 870324, Tuscaloosa, AL 35487-0324

and

L. Armus

California Institute of Technology, Pasadena, CA 91125

Received __________________; accepted __________________

Submitted to Astrophysical Journal (Letters).

ABSTRACT

We report a sensitive search for redshifted CO (3–2) emission from the weak radio galaxy 53W002 at z=2.394. Maps at resolutions of 3″ and 235 km s^{-1} show a significant emission peak within 0.5″ of the optical and radio continuum peaks. The measured narrow band flux is approximately ten times the extrapolated cm-wavelength non-thermal radio continuum expected at 101.9 GHz and exhibits a spectral profile implying a 540 km s^{-1} width (FWHM) at a systemic redshift z = 2.394 ± 0.001 for CO (3-2). This emission has a total integrated flux of 1.51 ± 0.2 Jy km s^{-1}, approximately 4 times weaker than that previously seen in the lensed systems FSC10214+4724 and the Cloverleaf QSO. For a Galactic CO-to-H_2 conversion ratio, the implied molecular gas mass is $7.4{\times}10^{10}$ $M_\odot$ (H_0 =75 km s^{-1} Mpc^{-1} and q_0 =0.5). The CO emission is elongated at PA = 120° with a deconvolved major axis radius of 15 kpc (2.8″). This extension is along a similar direction to that seen in the cm-wave radio continuum and the optical but approximately three times larger. A velocity gradient is seen along the major axis, and if this structure is a (forming) disk, the implied dynamical mass is 9-22$\times10^{10}$ $M_\odot$ at r $\leq$ 15 kpc, assuming inclination i = 0° (edge-on). The magnitude of these masses and the similarity of the high gas-mass fraction are consistent with the host galaxy of 53W002 being a young galactic system but the metallicity (probably $\geq 0.1 Z_\odot$ in order to produce the CO lines) implies significant heavy element production prior to z=2.4. This constitutes the first high redshift molecular gas which is detected in emission where there is probably no gravitational magnification.

Subject headings: galaxies: individual (53W002) – galaxies: active – ISM: molecules — galaxies: formation

1. Introduction

Early in the evolution of galaxies, there will be a phase in which the predominant mass component is interstellar and observations of this matter are critical to progress in understanding the initial building of galaxies and their stellar populations. Although the protogalactic gas should initially be atomic (or ionic), virtually all star formation models suggest that the gas becomes molecular during collapse to form stars. With relatively small metal enrichment ($\geq$ 10% solar metallicity) in a prior, low-level starburst, this denser ISM becomes observable in the CO rotational transitions at mm-wavelengths. To date, there have been three confirmed detections of CO emission at redshift $z \geq 1$: FSC10214+4724 at z=2.28 (Brown & Vanden Bout 1992, Solomon et al. 1992a, Scoville et al. 1995); the Cloverleaf QSO at z=2.56 (H1413+117 – Barvainis et al. 1994, Yun et al. 1997); and BR1202-0725 at z=4.69 (Ohta et al. 1996, Omont et al. 1996). In the first two (and possibly the last also, c.f. Omont et al. 1996), the high redshift system is gravitationally lensed by a foreground galaxy or cluster and the intrinsic (non-amplified) properties are therefore too uncertain for broad inferences about protogalactic evolution.

In this letter we report high resolution aperture synthesis observations designed to detect and image the molecular emission in the radio galaxy 53W002 and its associated galaxy group or cluster at z_{opt} = 2.390 (Windhorst *et al.* 1991, hereafter W91; Windhorst *et al.* 1994; Pascarelle *et al.* 1996a, 1996b). This cluster is clearly not subject to significant gravitational lensing based on the optical morphology and the fact that the separate galaxies have somewhat different redshifts and quite different spectra. 53W002 is unlikely to be lensed by the lower-luminosity z=0.581 elliptical galaxy that appears 5$''$ to its North-West (c.f., W91; Windhorst *et al.* 1992, 1994). Moreover, no other lensed images at z=2.39 are seen immediately surrounding this object in the narrow-band redshifted Lyα WFPC2 images of Pascarelle *et al.* (1996b). This radio-selected cluster was chosen for a sensitive

search for molecular emission since it appears to be a group of young, presumably gas-rich objects and Yamada *et al.* (1995) have reported a possible CO (1-0) emission feature here. Our observations clearly detect CO (3-2) emission (albeit at a level corresponding to a mass which is probably 5–14 times less than would be consistent with Yamada *et al.*). Throughout this letter, we adopt H_0 =75 km s^{-1} Mpc^{-1} and q_0 =0.5.

2. Observations

53W002 was observed using the Owens Valley Millimeter Array in three configurations between February 1996 and January 1997. The array consists of six 10.4 m telescopes, and the longest baseline observed was 242 m. For 53W002 whose systemic optical redshift is z=2.390 (see W91), the CO (3–2) transition occurs at 101.95 GHz. The synthesized beams were $2.39\times1.94''$ (uniform weighted) and $4.09\times2.96''$ (natural), both at PA=$-68°$. The phase center, central redshift for the measured CO line, and adopted angular size and luminosity distances for 53W002 are given in Table 1. The primary beam of the 10.4 m telescopes is $70''$ and thus the observations cover all objects in the cluster within $\sim35''$, corresponding to 150 kpc at 53W002. Several other z=2.4 candidates are included in this area : 5, 11, etc. of Pascarelle *et al.* (1996a, b). The system temperatures were typically 250–350 K in the signal side-band corrected for antenna and atmospheric losses and for atmospheric incoherence. Spectral resolution was provided by a digital correlator configured with 120×4 MHz channels (11.4 km s^{-1}), covering a total velocity range of 1,300 km s^{-1}. In addition, the continuum emission was measured in a 1 GHz bandwidth analog correlator. The total useable integration time on source was 61 hours distributed over 15 tracks in the three different telescope configurations. The nearby quasar 1828+487 (1.95 Jy at 102 GHz) was used to track the phase and gain variations, and Uranus (T_b=125 K) and 3C 454.3 were observed for absolute flux calibration. The positional accuracy of the resulting maps

is $\sim 0.3''$. The data were calibrated using the standard Owens Valley array program mma (Scoville et al. 1992) and mapped using DIFMAP (Shepherd et al. 1994) and the NRAO AIPS package. For the continuum maps (BW = 1 GHz), the rms noise was 0.20 and 0.48 mJy for natural and uniform weighting, respectively.

In order to predict more accurately the expected non-thermal radio continuum at 101.9 GHz, we also obtained 25 min of data with the NRAO VLA at 14.9 GHz in the B-array on March 11, 1997. 3C 286 and 1658+476 were used for flux and gain calibration. The synthesized beam is 0.81×0.53 $''$ (PA=–82°) for these data. The source was unresolved ($\leq 0.31''$ in diameter) with an integrated flux of 2.8 ± 0.1 mJy.

3. Results

In Figure 1 the interferometric spectrum integrated over the central $5''$ centered on 53W002 is shown, smoothed to a velocity resolution of 235 km s^{-1} and sampled every half resolution element. The peak flux is 3.1 ± 0.5 mJy and the deconvolved line-width is 540 ± 100 km s^{-1} (FWHM). For comparison, the peak flux of FSC10214+4724 is 14 ± 2 mJy and the full linewidth is 250 km s^{-1}(Scoville et al. 1995, Downes et al. 1995) and similar parameters hold for the CO emission from the Cloverleaf QSO (Barvainis et al. 1994); thus the emission in the unlensed radio galaxy 53W002 is more than a factor of four weaker than that in the previously detected high redshift systems.

In Figure 2 maps of the CO emission integrated over velocity ranges with ΔV=235 km s^{-1} are shown. In Figure 3 the total CO line flux integrated over 200 MHz (590 km s^{-1}) centered on the line is shown superposed on the HST V-band image from Windhorst, Keel, & Pascarelle (1997). The flux in the integrated CO map is 1.51 ± 0.2 Jy km s^{-1} and the peak flux in the channel maps is 4.06 ± 0.89 mJy beam^{-1}. No other CO emission features

were detected within our 70 $''$ primary beam. We can therefore set upper limits at ≤ 1.5 mJy (2σ) for the line flux at the positions of z=2.4 candidates 5, 11, etc of Pascarelle *et al.* (1996b).

The deconvolved size of the emission feature seen in the integrated map (Figure 3) is $5.7 \pm 1.3''$ by $1.7 \pm 0.7''$ (FWHM) with major axis at PA=114° . At the angular size distance of 1.08 Gpc, the major axis diameter corresponds to 29.9 kpc, or a radius of 15 kpc. In view of the limited signal-to-noise ratio in the maps, these size estimates are highly uncertain; however, it is clear that the emission is resolved since the centroid is shifted in the channel maps (see Figure 2) with positive velocity emission (relative to systemic) seen predominantly in the southeast and negative velocities in the northwest. The fact that this velocity gradient is along the major axis of the intensity distribution is suggestive of rotation, possibly in a forming disk.

The peak flux in the narrow band maps (4 mJy) implies a beam averaged brightness temperature excess of 39 mK at λ=2.9 mm or 0.13 K in the rest frame of the source. This corresponds to an absolute brightness temperature of 9.5 K in the rest frame after adding in the cosmic background radiation. No emission, above that expected due to the CO line, was detected in the 1 GHz (BW) continuum filter at a level $\sigma = 200$ μJy – the CO line contribution averaged over 1 GHz is expected to be ~ 0.5 mJy.

In Figure 4 the radio spectral energy distribution is shown, including the lower frequency fluxes of W91 and our measured flux at 15 GHz (2.8 ± 0.2 mJy) and the measured continuum at 101.9 GHz corrected for the known line flux. A power law fit to the radio continuum (dashed line) gives a spectral index $\alpha = 1.2 \pm 0.1$. The line flux, averaged over 200 MHz (2.8 mJy) is shown as the solid dot to indicate that it far exceeds the flux expected from extension of the cm-wavelength radio continuum, and hence it must be line emission. We also note that there is no evidence at 15 GHz for a significant thermal

nuclear component setting in at higher frequencies since this point lies on the power-law extrapolation of the lower frequency data. Scaling Arp 220 for the H2 mass and luminosity distance, the expected thermal dust emission for 53W002 at 102 GHz (345 GHz rest frame) is about 0.1 mJy, and the free-free emission would be 10-100 times less (c.f. Scoville *et al.* 1997).

4. Analysis and Discussion

The center frequency of the CO(3–2) emission is 101.86 GHz, corresponding to a mean redshift of z=2.394±0.001. This is marginally different (350 km s^{-1}) from the mean redshift z=2.390±0.001 for the optical/UV emission lines (W91, Pascarelle *et al.* 1996a, b). A similar offset with higher redshifts for the radio versus optical lines has been noted for lower redshift, high luminosity galaxies (Mirabel & Sanders 1989). The offset might be explained if molecular gas and dust gas is falling into the galaxy, or if the optical/UV lines originate from gas flowing out of the galaxy with the symmetric redshifted emission extincted by dust within the system.

From the integrated line flux of 1.51±0.2 Jy km s^{-1}, we obtain a total CO (3-2) luminosity of L'_{CO}=1.86×10^{10} K km s^{-1} pc^2, using equation (3) from Solomon et al. (1992b). (This is a factor of 3 weaker than that of FSC10214+4724.) For a Galactic conversion factor α=4 $M_\odot$ (K km s^{-1} $pc^2)^{-1}$, the total molecular mass is 7.4×10^{10} $M_\odot$. The limits on the mass from other objects within the primary beam (eg. objects 5, 11, etc) are $\leq 3\times10^{10}$ $M_\odot(2\sigma)$. If the clouds are hotter or denser than Galactic GMC's, as would be expected in a vigorous starburst galaxy, the conversion factor should vary as $n^{1/2}/T_{CO}$. To some extent, the decrease in the conversion factor due to the hotter gas may be offset by increased density. In Arp 220, an independent dynamical constraint on the conversion factor suggests a value $\sim$ 0.45 times the Galactic value (Scoville, Yun, & Bryant 1997).

Based on the measured sizes and line-widths, it is also possible to estimate the dynamical mass associated with the CO emission feature. Assuming the galaxy is rotating, $M_{dyn} = RV_{1/2}^2/Gsin^2 i$. For $V_{1/2}$, we adopt 200–250 km s^{-1}, i.e. approximately half of the measured line width, and we take R= 10–15 kpc; we then obtain 0.9–2.2$\times10^{11}$ M$_\odot$ for the galaxy, with no correction for inclination. The molecular gas mass, assuming the Galactic CO-to-H_2 conversion factor, would therefore constitute between 30–80% of the total dynamical mass.

In present epoch galaxies, the gas mass fraction is typically $\leq$ 10%; the probably much higher values indicated for 53W002 are consistent with this being a genuinely young galaxy, still in its initial phase of star formation. In nearby ultraluminous IRAS galaxies, high gas mass fractions are also indicated (cf. Scoville, Yun, & Bryant 1997), but in these cases the gas is concentrated almost entirely in the central kpc – not over 30 kpc as in 53W002. Based on rest frame UV data for 53W002, W91 and Windhorst *et al.* (1997) have derived star formation rate of 50-100 $M_\odot$yr^{-1} in order to account for the fluxes and colors. The age of the stellar population is estimated by them to be 0.3-0.5 Gyr in the center and 0.5-1 Gyr at $\sim$ 10 kpc radius. At these rates, the estimated mass of molecular gas would be cycled into stars within $\sim 10^9$ yrs; this is also consistent with a young age for the system.

53W002 also has a weak extension in the optical to the West ($\sim$ 4 kpc; Windhorst *et al.* 1997) which may be seen in the HST B- and V-band images (see Figure 3). The east-west orientation of this feature is similar to that of the radio source (cf. Windhorst et al. 1991) and the CO emission although the latter is extended on both sides of 53W002.

Yamada *et al.* (1995) have reported detection of a possible CO (1-0) feature from 53W002 at a central redshift z = 2.392 with peak and integrated fluxes of 5 mJy and 1.92 Jy km s^{-1}; however, it seems unlikely that this is the CO (1-0) counterpart of the CO (3-2) emission reported here in view of the much lower mass implied by our CO (3-2) flux

(and the marginally different redshift). For optical thick CO emission lines with the same brightness temperature in both CO transitions, the (3-2) flux should be 9 times greater (if the lines are optically thin, the ratio should be higher still). For low excitation GMC's in the Galactic disk, the line temperature ratios are typically (1-0) : (2-1) : (3-2) = 1 : 0.7 : 0.4 (Sanders et al. 1997). Thus even in the case of optically thick Galactic clouds, our line flux is approximately a factor of 5 weaker than what would be expected from the Yamada *et al.* feature, and in the more likely case of nearly equal brightness temperatures, it is a factor ∼14 weaker. Lastly, it is possible that Yamada *et al.* have detected additional flux from the other 18 z=2.4 objects of Pascarelle *et al.* (1996b) in the vicinity of 53W002; however, our maps show no other comparably strong features within an area larger than their 50″ diffraction beam. CO emission was not detected by us from the other objects in the interferometer field of view (70″) at levels less than 1/3 of that seen in 53W002. These systems must have less massive ISM's than the galaxy associated with 53W002. The CO luminosity of 53W002 is approximately three times that of the nearby ultraluminous IRAS galaxy Arp 220 (cf. Scoville, Yun, & Bryant 1997) and is similar to the most gas-rich local systems such as IR14348-14 (Sanders et al. 1991) and the radio galaxy PKS1345+12 (Mirabel & Sanders 1989, Evans et al. 1996).

The large gas-mass found for 53W002 suggests that this is a very gas-rich and massive young galaxy – perhaps the progenitor of an elliptical or early-type spiral galaxy. In the course of its subsequent dynamical evolution, the gas in 53W002 may concentrate in the center (through dissipative energy loss as is likely to have happened in the nuclei of the nearby ultraluminous IRAS galaxies, cf. Scoville et al. 1994). The central mass density could then become high enough to place the system in the area of the fundamental plane occupied by present-epoch elliptical galaxies (Kormendy & Sanders 1992). Already, the light profile in the envelope at radii 6–9 kpc apparently follows an $r^{1/4}$ law (Windhorst *et al.* 1992, 1994b, Windhorst *et al.* 1997), for which W91 derived a luminous mass of

$2 - 4 \times 10^{11}$ $M_\odot$ from nine-band photometry combined with its spectra. Lastly, we note that 53W002 is a compact steep spectrum radio source and at the present epoch, such radio sources are hosted usually by elliptical galaxies.

In conclusion, we may be witnessing the birth of a luminous elliptical or early-type spiral galaxy. The copious amount of CO (and H_2) gas detected with OVRO suggest that such formation may have initially been associated with a massive disk, that is subsequently destroyed by mergers or tidal effects, eventually to leave a luminous bulge-dominated galaxy.

The Owens Valley millimeter array is supported by NSF grants AST 93-14079 and AST 96-13717. The HST observations were supported by NASA grants GO-5308.*.93A and GO-5985.*.94A (to RAW and WCK) from STScI, which is operated by AURA, Inc., under NASA contract NAS5-26555. N. Scoville thanks Don Hall and Dave Sanders for hospitality at the Institute for Astronomy, University of Hawaii when part of this work was done. We also thank Aaron Evans for comments and suggestions on the manuscript.

Table 1. Summary of CO Observations and Derived Properties

RA (B1950)	$17^h12^m59\overset{s}{.}86$
DEC (B1950)	$+50°18'51\overset{''}{.}3$
$< z >_{CO}$	2.394 ± 0.001
Luminosity Distance[a]	12.41 Gpc
Angular-Size Distance[a]	1.08 Gpc (1″ → 5.24 kpc)
M_{H_2}[b]	$(7.4 \pm 1.5) \times 10^{10}$ $M_\odot$
$M_{dyn} sin^2 i$	$(9 - 22) \times 10^{10}$ $M_\odot$

[a] $H_o = 75$ km s^{-1} Mpc^{-1}, $q_o = 0.5$

[b] using α=4 $M_\odot$ (K km s^{-1} pc^2)$^{-1}$

REFERENCES

Barvainis, R. Tacconi, L., Antonucci, R. & Coleman, P. 1994, Nature, 371, 586

Brown, R., & VandenBout, P. 1992, ApJ, 397, L19

Downes, D., Solomon, P. M. & Radford, S. E. 1995, ApJ, 453, L65.

Evans, A. S. *et al.* , 1996, ApJ, 457, 658

Kormendy, J. & Sanders, D. B. 1992, ApJ, 390, L53

Mirabel, I. F. and Sanders, D. B. 1989, ApJ, 340, 253

Ohta, K., Yamada, T., Nakanishi, K., Kohno, K., Akiyama, M. & Kawabe, R. 1996, Nature, 382, 426

Omont, A., Petitjean, P., Guilloteau, S., McMahon, R. G. & Solomon, P. M. 1996, Nature, 382, 428

Pascarelle, S. M., Windhorst, R. A., Driver, S. P., Ostrander, E. J, & Keel, W. C. 1996, ApJ, 456, L21

Pascarelle, S. M., Windhorst, R. A., Keel, W. C., & Odewahn, S. C. 1996, Nature, 383, 45-50

Sanders, D. B., Scoville, N.Z., & Soifer, B. T. 1991, ApJ, 370, 158

Sanders, D. B., Carpenter, J., Tilanus, R., Deane, J. & Scoville, N. 1997,ApJ, in preparation

Scoville, N. Z., Carlstrom, J. C., Chandler, C. J., Phillips, J. A., Scott, S. L., Tilanus, R. P., & Wang, Z. 1992, PASP, 105, 1482

Scoville, N. Z., Hibbard, J. E, Yun, M. S., & van Gorkom, J. H. 1994, in *Mass Transfer Induced Activities in Galaxies,* ed. I Shlosman (Cambridge University Press: Cambridge)

Scoville, N. Z., Yun, M. S., Brown, R. L. & VandenBout, P. A. 1995, ApJ, 449, L109

Scoville, N. Z., Yun, M. S. & Bryant, P. 1997, ApJ, in press

Shepherd, M. C., Pearson, T. J., & Taylor, G. B. 1994, BAAS, 26, 987

Solomon, P. M., Downes, D., & Radford, S. J. E. 1992a, Nature, 356, 318

Solomon, P. M., Downes, D., & Radford, S. J. E. 1992b, ApJ, 398, L29

Windhorst, R. A., Burstein, D, Mathis, D. F., Neuschaefer, L. W., Bertola, F., Buson, L. M., Koo, D. C., Matthews, K., Barthel, P. D., & Chambers, K. C. 1991, ApJ, 380, 362 (W91)

Windhorst, R. A., Mathis, D. F., & Keel, W. C. 1992, ApJ, 400, L1 (W92)

Windhorst, R. A., Gordon, J. M., Pascarelle, S. M., Schmidtke, P. C., Keel, W. C., Burkey, J. M., & Dunlop, J. S. 1994b, ApJ, 435, 577 (W94b)

Windhorst, R. A., Keel, W. C., & Pascarelle, S. M. 1997, ApJ, resubmitted

Yamada, T., Ohta, K., Tomita, A., & Takata, T. 1995, AJ, 110, 1564

Yun, M. S., Scoville, N. Z., Carrasco, J. J., & Blandford, R. D. 1997, ApJ, 479, L9

This manuscript was prepared with the AAS LaTeX macros v4.0.

Fig. 1.— Average spectrum of CO (3–2) emission in 53W002 smoothed to 80 MHz (235 km s^{-1}) resolution is shown for a $5''$ aperture centered on the position of 53W002.

Fig. 2.— Maps of the CO emission in 53W002 averaged over 235 km s^{-1} velocity ranges are shown as a function of coordinate offset from the phase center. The cross marks the position of the 15 GHz continuum peak (see Table 1). The contours are -3, -2, $+2$, $+3$, $+4$, & $+5$ times 0.89 mJy beam^{-1} (1σ), and the natural weighted beam is shown. The velocities are relative to z=2.394. No significant continuum emission was detected (see §3).

Fig. 3.— The CO (3–2) emission is shown integrated over all channels containing significant line emission (v=-270 to $+270$ km s $^{-1}$). On the right panel, the $4 \times 4''$ area immediately surrounding the radio continuum peak (cross) is shown zoomed in, with the CO emission contours superposed on the HST V-band image (Windhorst *et al.* 1997). The CO contours correspond to -3, -2, $+2$, $+3$, $+4$, and $+5$, times 0.44 mJy beam^{-1} (1σ).

Fig. 4.— The radio continuum spectrum of 53W002 is shown with points at 101.9 GHz to indicate the measured peak CO (3-2) line flux (solid dot = 2.8 mJy averaged over 200 MHz), the flux measured in the 1 GHz BW continuum filter and the latter corrected for the CO line flux averaged over the 1 GHz filter. The last, shown as the solid triangle, provides an upper limit to the true continuum at 101.9 GHz (i.e. 0.3±0.2 mJy). The radio fluxes are from Windhorst *et al.* (1991) (600 MHz, 1.4 GHz, 8.4 GHz) and this article (15 GHz). The dashed line is a power law with $\alpha = 1.2$ fit to the cm-wave data; the measured narrow band line flux at 101.9 GHz is far above the extrapolated radio continuum.

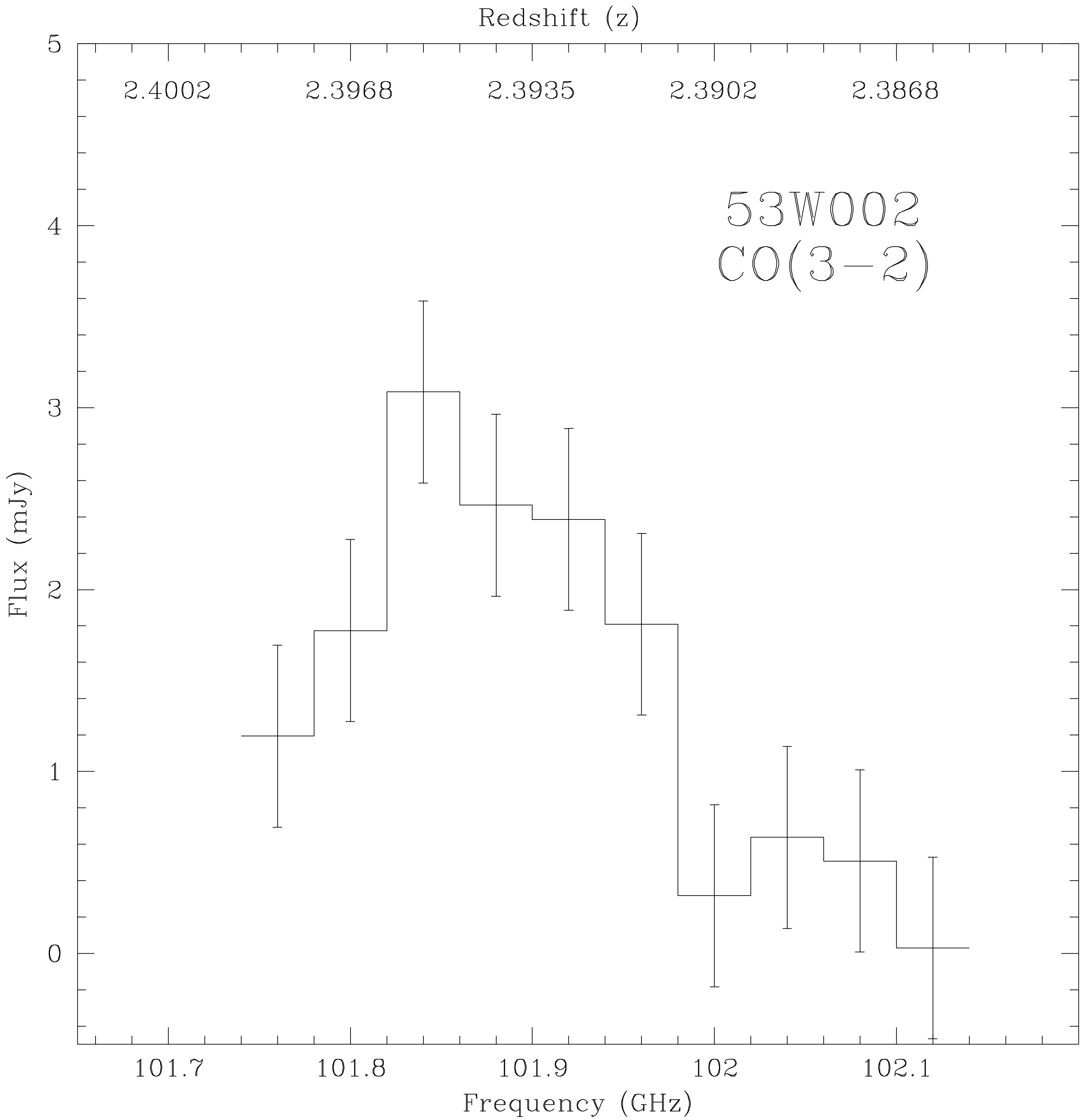

Redshift (z)
2.4002
2.3968
2.3935
2.3902
2.3868
53W002
CO(3-2)
Flux (mJy)
5
4
3
2
1
0
101.7
101.8
101.9
102
102.1
Frequency (GHz)

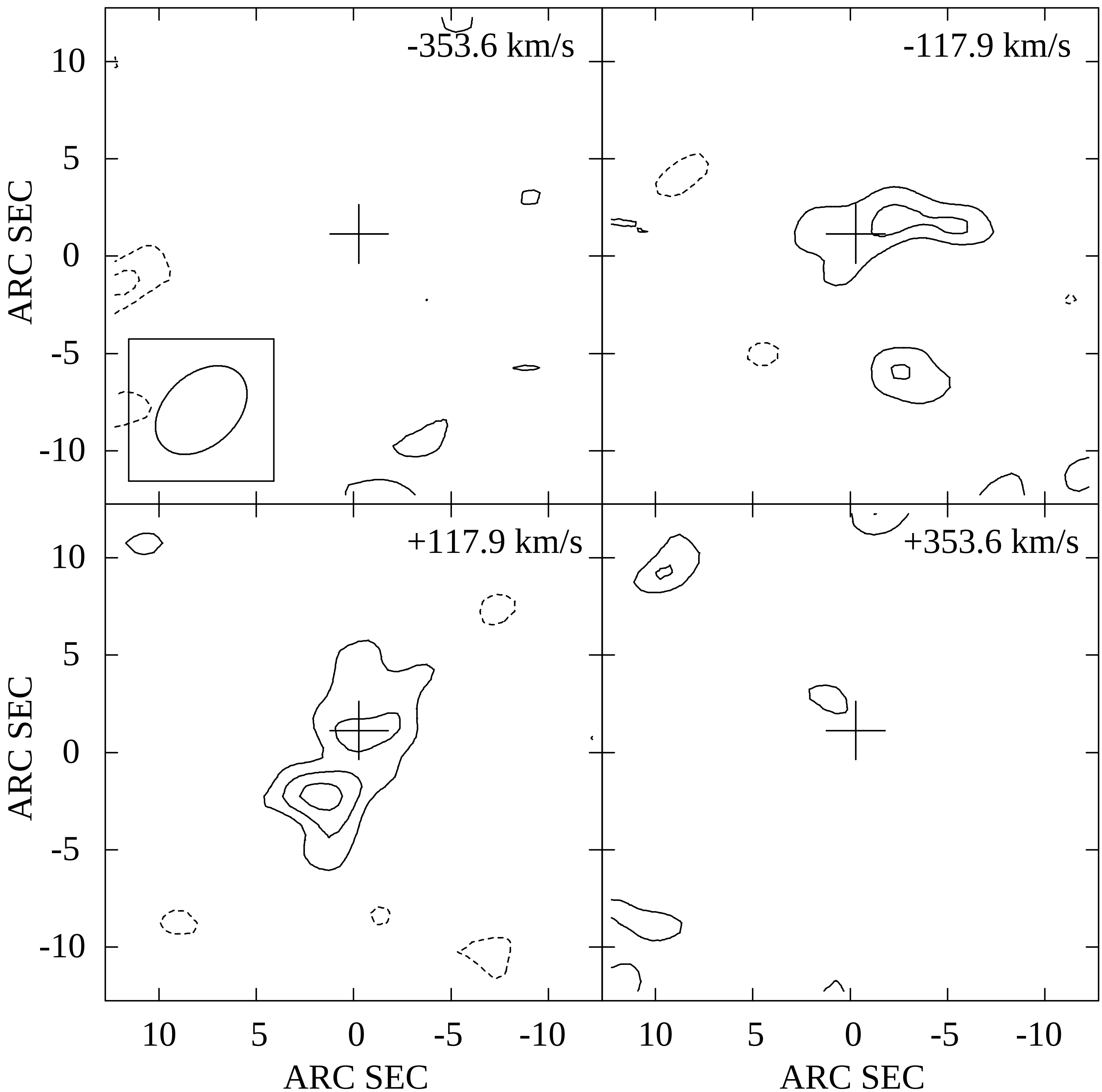
-353.6 km/s
-117.9 km/s
+117.9 km/s
+353.6 km/s
ARC SEC
ARC SEC
ARC SEC
ARC SEC
10
5
0
-5
-10

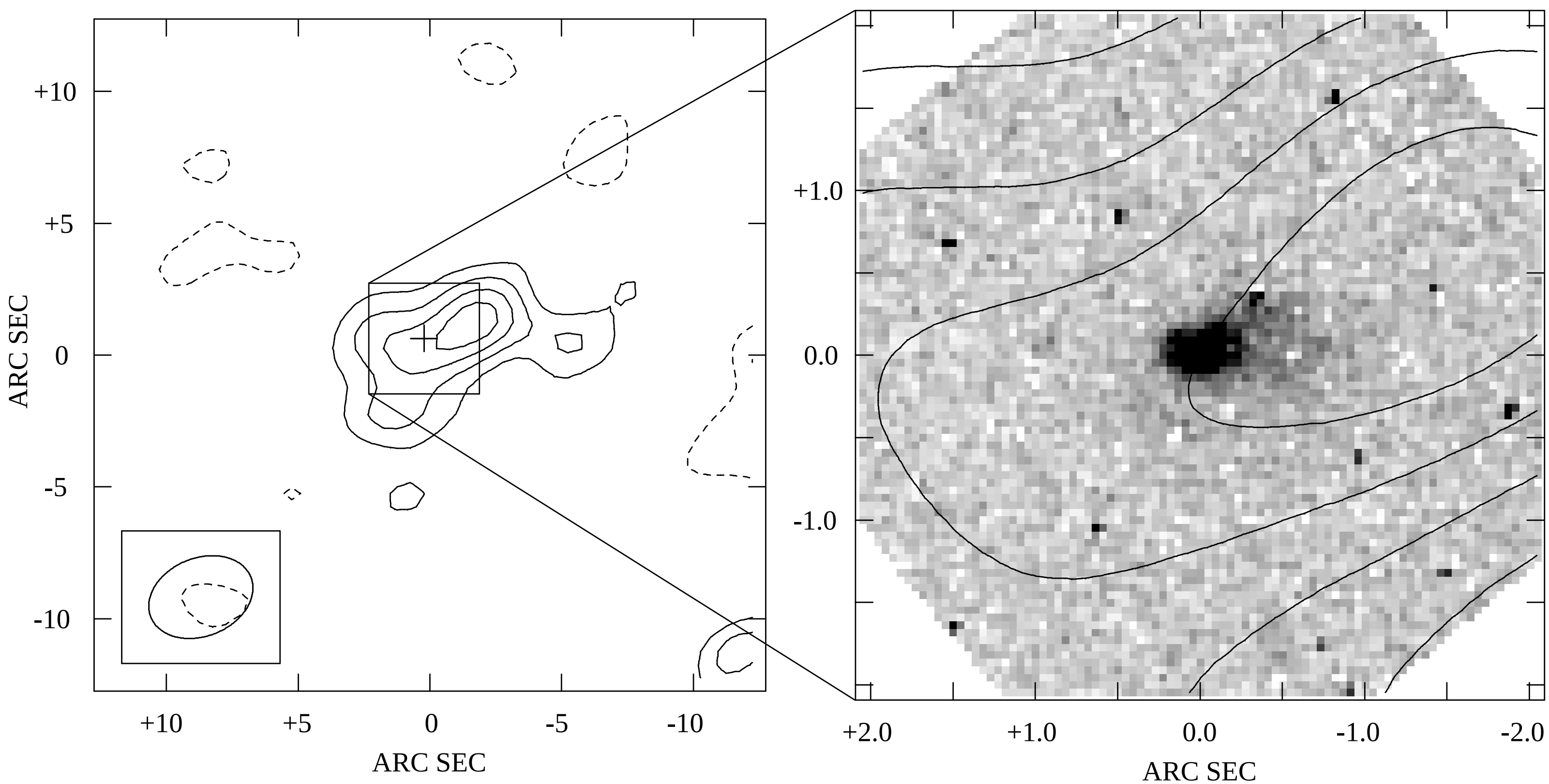

+10
+5
0
-5
-10
ARC SEC
ARC SEC
+1.0
0.0
-1.0
+2.0
+1.0
0.0
-1.0
-2.0
ARC SEC

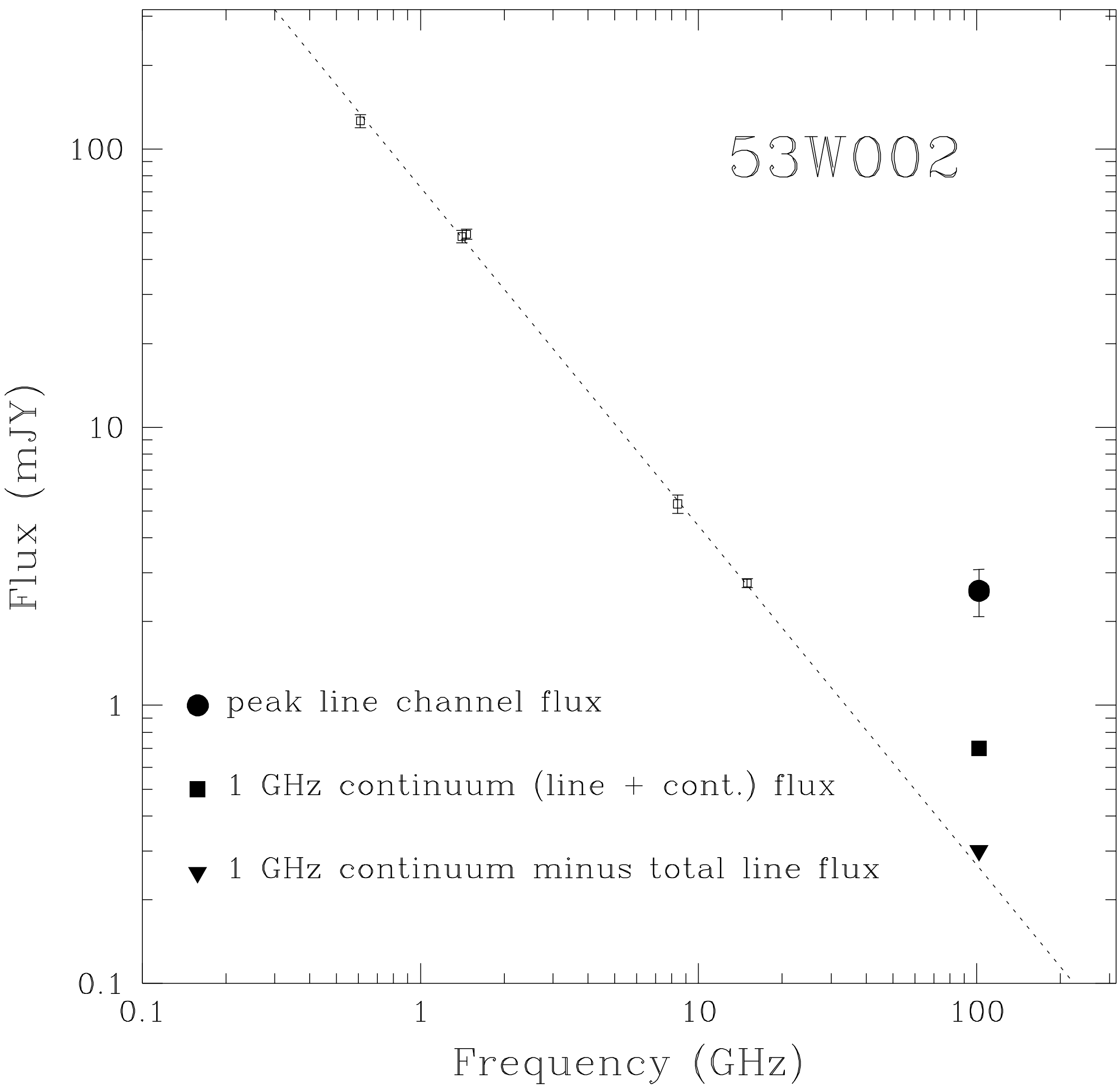

53W002
Flux (mJY)
Frequency (GHz)
0.1
1
10
100
peak line channel flux
1 GHz continuum (line + cont.) flux
1 GHz continuum minus total line flux